The Bernese Multibeam Radiometer for KOSMA (BEMRAK) – Instrument Design and First Antenna Measurements

Thomas Lüthi, Andreas Lüdi, Axel Murk, Aleksandar Đurić, and Andreas Magun

Research Report No. 2003-05

Institute of Applied Physics — Dept. of Microwave Physics

Sidlerstr. 5
CH-3012 Bern
Switzerland

Tel. +41 31 631 89 11
Fax. +41 31 631 37 65
E-mail iapemail@iap.unibe.ch

Abstract

The Bernese Multibeam Radiometer for KOSMA (BEMRAK) is a 210 GHz multibeam receiver for solar flare observations that will be integrated into the KOSMA submillimeter telescope on the Gornergrat. It will provide accurate source positions and an estimate of source sizes, thus allowing absolute flux-density calibrations at 210 GHz as well as for the already available 230 and 345 GHz channels of KOSMA.

Due to delivery problems of the feedhorns and mixers, as well as a pending repair of the 230/345 GHz receiver, final integration into the telescope will not be possible before mid-June 2003. In order to gain preliminary test results for the design a single channel was used. The near field in the focal plane of the feed assembly, consisting of a corrugated horn and an elliptical mirror was measured in the laboratory and compared to results from modelling. Finally, the antenna beam patterns of the telescope were measured in the far field by means of a test transmitter.

The results clearly show that the receiver design performs as expected, so that no further modifications are needed.

Contents

1 Introduction

On April 12, 2001, a solar flare was detected for the first time at frequencies up to 345 GHz with the 3 m telescope of the Köln Observatory for Submillimeter and Millimeter Astronomy (KOSMA) on the Gornergrat. Although atmospheric conditions were very favourable with low opacity ($\tau_0 \sim 0.48$ at 345 GHz) and low atmospheric transmission fluctuations ($\sim$1%), flux density calibration turned out to be very difficult as the source position of the flare relative to the antenna beam direction was not known well enough [12, 14].
Source positions can be obtained from solar maps, but the resulting time resolution decreases to several minutes, which is not acceptable for solar flare observations (appendix A). In order to measure accurate source positions with millisecond time-resolution and to obtain an estimate of the source size a multibeam receiver for the KOSMA-telescope was designed: The **Be**rnese **M**ultibeam **Ra**diometer for **K**OSMA (BEMRAK).

2 Solar Flare Observations with a Multibeam Telescope

As already described in many papers (e.g. [2, 7, 11, 3]) a multibeam antenna can be used to determine the angular position of a point like burst source with at least 3 beams. This is done by pointing them into slightly different directions and by measuring the different source intensities. Source positions are reconstructed by calculating the theoretical intensity ratios for an assumed source position and known antenna patterns. From comparison with the measured intensity ratios the source position is found with an accuracy of up to two orders of magnitude better than the antenna HPBW. The noise-induced errors of the reconstructed source position are minimum for beams intersecting at the -3 dB-level [9].
When the source is observed with at least 4 beams simultaneously also an estimate of the source size can be obtained [1]. The measured signal I_i in each channel is proportional to the convolution of the antenna pattern P_{ni} and the source brightness temperature distribution T_B:

$$\begin{aligned} I_i &\propto P_{ni} \otimes T_B \\ &= I_i(\vartheta_s - \vartheta_i, \varphi_s - \varphi_i, HPW_s, S), \end{aligned} \tag{1}$$

where (ϑ_s, φ_s) and (ϑ_i, φ_i) are the positions of the source and beam i respectively, HPW_s the half power width and S the total flux density of a circular source with a Gaussian shape. For four antenna beams with known antenna patterns that point

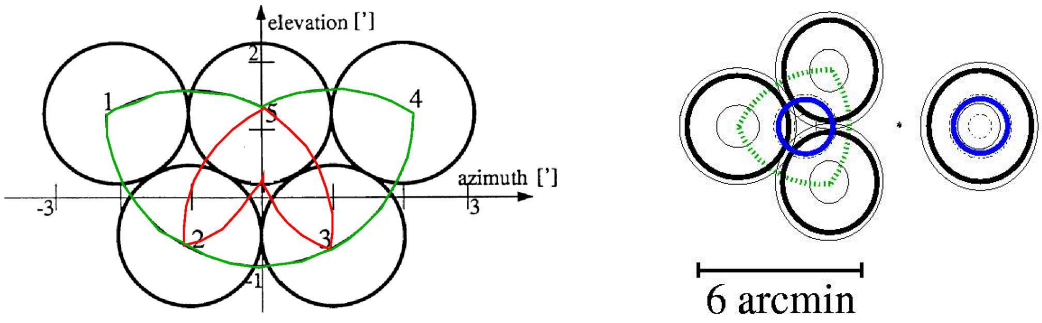

Figure 1: -3 dB contours of the Itapetinga (48 GHz, [7]) and SST-telescope (212 and 405 GHz, [9]). Unambiguous localisation of point sources is possible within the green areas, estimation of the source size within the red one (Itapetinga only).

to slightly different directions, we obtain

$$\frac{I_i}{I_{j\neq i}} = \frac{I_i(\vartheta_s - \vartheta_i, \varphi_s - \varphi_i, HPW_s, S)}{I_{j\neq i}(\vartheta_s - \vartheta_{j\neq i}, \varphi_s - \varphi_{j\neq i}, HPW_s, S)}, \qquad i,j = 1...4. \tag{2}$$

This equation is solved numerically with the measured far-field patterns to obtain the source position (ϑ_s, φ_s) and its diameter HPW_s. Knowing these parameters and the antenna patterns, the total flux density of the flare S can be calculated from the observed intensities.

Due to the contribution of sidelobes to the measured intensity, reconstruction of the source position and size is unambiguous only in a limited area [10]. Figure 1 shows the -3 dB contours of the two multibeam telescopes in use today for solar flare observations, namely the Itapetinga-telescope (left side) and the solar submillimeter telescope (SST) in El Leoncito (right side). Unambiguous reconstruction of the source position assuming a point source is possible within the green areas.

The five beams of the Itapetinga-telescope also allow an estimate of the source size for sources within the red area [1]. This area is considerably smaller than the area for three-beam position reconstruction, as the fourth beam is far away from the barycentre of the other three so that sidelobes can lead to ambiguities. In order to overcome this problem, BEMRAK's fourth beam will be placed at the centre of the other three beams (Fig. 2). This is achieved by installing only three feedhorns and synthesising a fourth beam from the other three. As the feedhorns and mixers are the most costly part of a radiometer, this is also a very cost-effective way to realise a four-beam instrument.

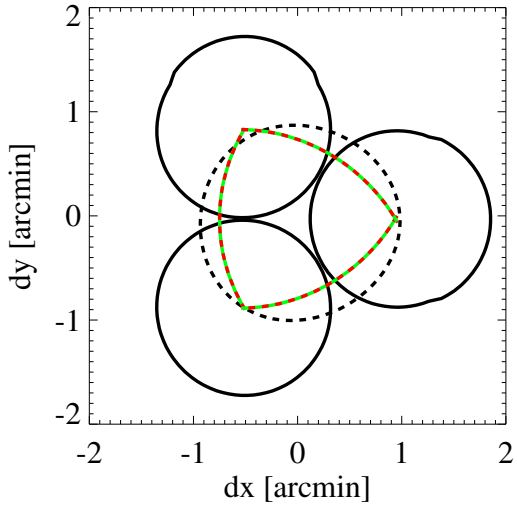

Figure 2: -3 dB contours of BEMRAK at 210 GHz. The synthesised fourth beam is indicated by the dashed contour line. Unambiguous reconstruction of source position and size is possible in the same (red/green striped) area as three-beam reconstruction of the source position. The KOSMA-beams at 230 and 345 GHz, that are centred on the 210 GHz beam cluster are not shown.

3 Instrument Design

As mentioned above, BEMRAK consists of three receivers at $\sim$210 GHz with their beams pointing into slightly different directions and intersecting at the -3 dB-level. Additionally, a fourth beam is synthesised from the other three, providing also an estimate of the source size. Assuming the source position to be frequency-independent, also the observed fluxes at 230 and 345 GHz can be corrected.

3.1 Quasioptics

BEMRAK will be integrated into the existing 230/345 GHz SIS-receiver of the KOSMA-telescope (Fig. 3). Before entering the different receivers the mm signal is split by a wire grid that is oriented under an angle of 45 degrees relative to the support plate. The reflected component is focused by an elliptical mirror into the three 210 GHz feedhorns of the multibeam receivers. The transmitted 230 and 345 GHz signals, linearly polarised under 135 degrees, are fed to the two receivers that are vertically and horizontally polarised. Although this results in

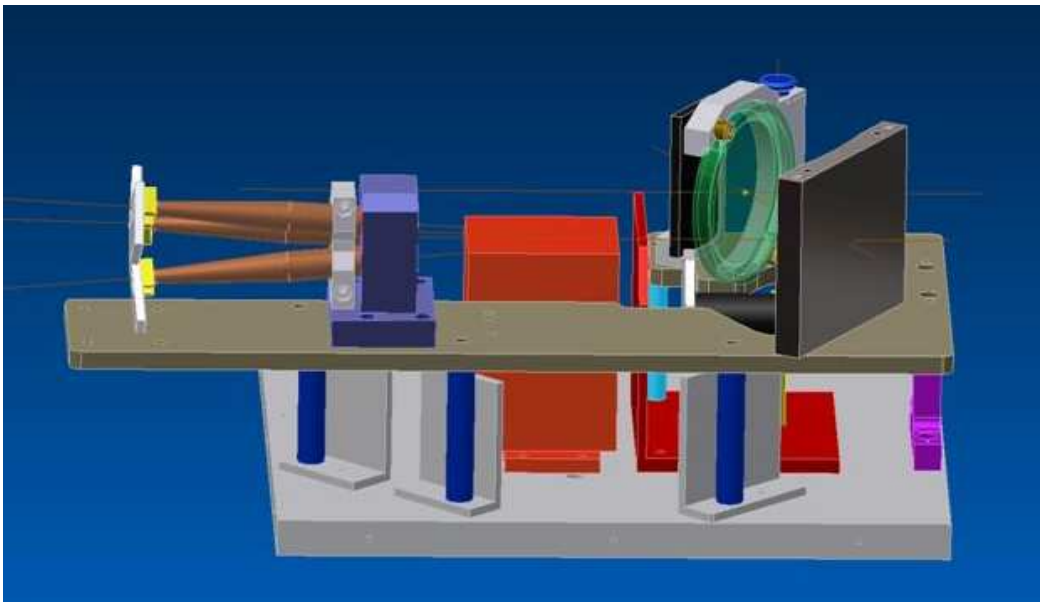

Figure 3: CAD-drawing of BEMRAK. The support plate of BEMRAK (brown) is mounted by pillars (blue and violet) on the light grey base plate of the KOSMA receivers at 230 and 345 GHz (red and orange). Radiation from the telescope is reflected by the wire grid (green) and focused by the elliptical mirror (dark grey) into the three feedhorns (copper). Not shown are the mixers and the front-end electronics.

a power reduction by -3 dB for the latter, the sensitivity for solar observations is barely affected due to the low receiver noise temperature ($\sim$100 K) which is orders of magnitude smaller than the antenna temperature during solar observations ($\sim$6000 K). The signal reduction is in fact a very welcome side effect for reducing receiver non-linearities.
In order to generate the intended antenna pattern directions (Fig. 2) the beams in the focal plane of the telescope must be $\sim$parallel and lie in the corners of an equilateral triangle. The positions of the feedhorns can therefore be determined by geometrical ray-tracing of the intended beams in the focal plane through the grid and elliptical mirror, leading to the skew angles of the feedhorns visible in Figure 3. All geometrical properties are specified in Appendix B.

3.2 Beam Synthesis

Figure 4 shows a schematic of BEMRAK: Beam synthesis is achieved by splitting the IF signals of each radiometer chain in two parts, of which one is detected

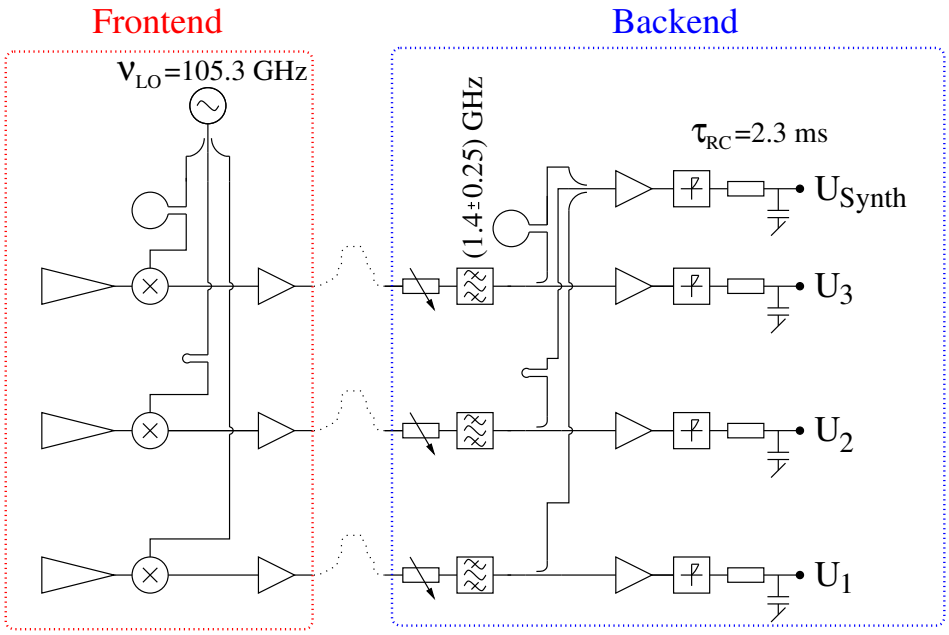

Figure 4: Schematic of BEMRAK's front and backend: All three mixers are (subharmonically) pumped by a common local oscillator in order to have a common phase information. The IF signals of each radiometer chain are splitted in two and then combined in order to synthesise a fourth beam (U_{Synth}). Electrically switchable attenuators provide enough dynamic range to avoid saturation even during very strong solar flares.

directly (U_1 to U_3) and the others are combined prior to detection (U_{Synth}). As beam synthesis requires all signals to have a common phase, the three mixers are pumped by a common local oscillator. Simulations with the General Antenna Program (GAP) from Comsat Laboratories showed that the signals of the three radiometer chains must be in phase within $\sim$60 degrees in order to obtain a usable synthesised beam. Phase correction must be done separately for the RF/LO and IF parts of the instrument: For RF-signals in the upper sideband phase differences are preserved during the mixing-process, in the lower sideband however there occurs a change of sign [12]. As BEMRAK operates in double sideband mode, phase differences in the RF/LO part can not be corrected at the intermediate frequency level for both sidebands simultaneously. Therefore phase correction will be accomplished by inserting delays into the appropriate signal paths. It will be checked by using a vector network-analyser to compare the phase of two IF-signals at a time, at first for the IF-part alone and then including the RF-part with a source at the observation frequency.

However, there are two problems that might affect our ability to synthesise a fourth beam:

- The seven amplifiers used in BEMRAK are of six different types. Should they or the other components introduce too large dispersion differences into the three radiometer chains, then it is not possible to meet the 60 degree phase error limit any more.
- The local oscillator used in BEMRAK offers just enough power for all three mixers, including the losses of an isolator, a power splitter and the waveguides. If however the mixers turned out to need more LO-power than specified, it would become necessary to use two phase-locked oscillators.

3.3 Sensitivity

The radiometric sensitivity of a radio telescope is

$$\Delta T = \frac{T_A + T_R}{\sqrt{2\Delta\nu\tau_{RC}}}, \tag{3}$$

where $\Delta\nu$ is the bandwidth and τ_{RC} the integration time. The receiver noise temperature T_R can be calculated from the mixer and amplifier noise temperatures and their respective losses and gains. The components envisaged for BEMRAK result in a receiver noise temperature of ∼3000 K, which could be validated with first laboratory measurements. The antenna temperature T_A follows from the equation of radiation transfer:

$$T_A = T_{B\odot} e^{-\tau_0/\sin(\theta)} + T_{atm}(1 - e^{-\tau_0/\sin(\theta)}) \tag{4}$$

The quiet sun brightness temperature $T_{B\odot}$ at a frequency of 210 GHz is ∼ 6400 K [4], and for the temperature of the atmosphere T_{atm} a value of 300 K is assumed. During summer time a zenith opacity τ_0 better than 0.3 is measured for ∼70% of the time ($\hat{\approx}$4 mm precipitable water vapour) and a value of 0.2 at 210 GHz is not unusual [8]. The elevation angle θ of the sun reaches values in excess of 65 degrees in the summer months. Assuming an elevation of 45 degrees and τ_0 = 0.2, equation 4 yields an antenna temperature of ∼5000 K.
With an integration time of 2.3 ms (the same as for the 230 and 345 GHz KOSMA receivers) and a DSB-bandwidth of 1 GHz the radiometric sensitivity is ∼3.7 K.
The quiet sun flux density collected by the 210 GHz antenna beams is $S_{\odot det}$ = 234 sfu[1]. The radiometric sensitivity in solar flux units then becomes

$$\begin{aligned} \Delta S_{radiom} &= \frac{\Delta T}{T_A} S_{\odot det} \\ &\approx 0.17 \text{ sfu.} \end{aligned} \tag{5}$$

[1] 1 sfu = 10^{-22}Wm^{-2}Hz^{-1}

Atmospheric conditions at Gornergrat are very favourable, but the sensitivity of the instrument will still be limited by the stability of the earth's atmosphere: During the April 12, 2001 flare the weather was very good with a zenith opacity of $\sim$0.18 at 230 GHz and flux-density fluctuations in the order of $\Delta S/S \approx 1\%$. Assuming similar effects at 210 GHz a sensitivity of $\sim$2.3 sfu can be expected.
In order to avoid detector saturation during strong solar flares[2], BEMRAK is equipped with electronically switchable attenuators in the IF-chains, automatically increasing attenuation when a certain threshold is reached.

4 First Measurements

By the end of February 2003 the fabrication of the mechanical parts as well as of the front- and backend electronics was finished, but, due to delivery problems, only one mixer and a single sample feedhorn (slightly damaged during the fabrication process; see below) were available. As the 230/345 GHz receiver, providing the mechanical support for BEMRAK, is to be returned to Köln for maintenance between early May and mid-June it will not be available for tests when the missing parts are scheduled to arrive. In order to test the receiver optics, system integration and preliminary antenna measurements with only one beam at a time were made on the 4th and 5th of March, 2003.

4.1 Feedhorns

The feedhorns for BEMRAK are corrugated with sine-tapered walls. They have a designed HPBW of 7.6 degrees, corresponding to a beam-waist of 4.03 mm. The tapered walls ensure that the beam-waist lies in the aperture-plane of the feedhorn. Due to a fabrication problem the feedhorns were visibly damaged. Nevertheless they were given to us as samples and their amplitude and phase patterns were measured with our vector network analyser from AB-Millimetrique. Fortunately at least one of them worked well enough to carry out preliminary focal plane and antenna pattern measurements. The results of the feedhorn pattern measurements (far field) are summarised in Figure 5. Besides a negligible sidelobe asymmetry, the H-plane pattern is $\sim$10% broader than in the E-plane. Above -13 dB there is a good agreement between the modelled and measured E-plane patterns. However, it should be kept in mind that some of the asymmetry-effects observed in the focal plane and antenna pattern measurements might well be due to mechanical asymmetries present in the feedhorn.

[2]This happened to the solar submillimeter telescope (SST) during the August 25, 2001 flare, when the 212 GHz channels were saturated by a flux density of at least 10000 sfu (J. P. Raulin, private communication).

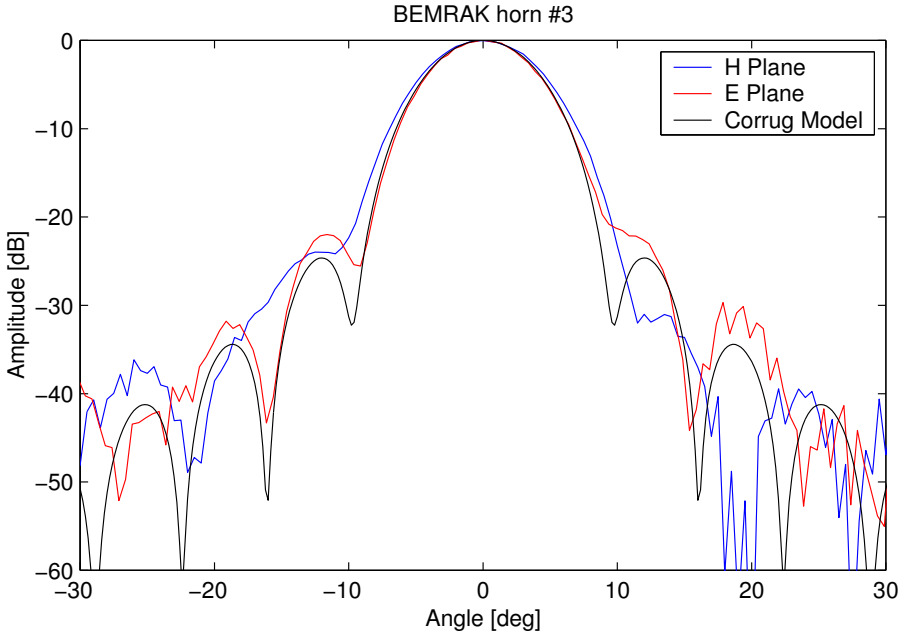

Figure 5: Measured and modelled (Thomas Keating Ltd, Richard Wylde) far-field patterns of the sample feedhorn.

Probably due to internal reflections and/or attenuation the receiver noise temperature increased to ∼30000 K when the sample feedhorn was mounted.

4.2 Focal plane pattern

The results from numerical simulations of the far-field beam patterns with GAP are in excellent agreement with the designed beam offsets and diameters. However, there were unexpected and doubtful features found in the field distribution along the focal plane of the telescope (behind the elliptical mirror). Especially beam 1 showed a strong asymmetry that could hardly be explained from physical reasons (Fig. 6). Therefore we had the power patterns in the focal plane also calculated by Microwave And Antenna Systems (Pat Foster) with the program REFLECT [5]. The quasi-optical design with fundamental Gaussian beams [6] and the simulations with GAP and REFLECT, give identical beam positions. The designed waist radii are 3.6 mm, whereas the simulations show a slightly higher value of ∼4.3 mm.
It is therefore of considerable interest to measure the patterns in the focal plane of the telescope. This was accomplished with the ABMM network-analyser and a planar xy-scanner with a waveguide-probe. Due to mechanical difficulties these preliminary measurements could only be carried out at a distance ∼15 mm away

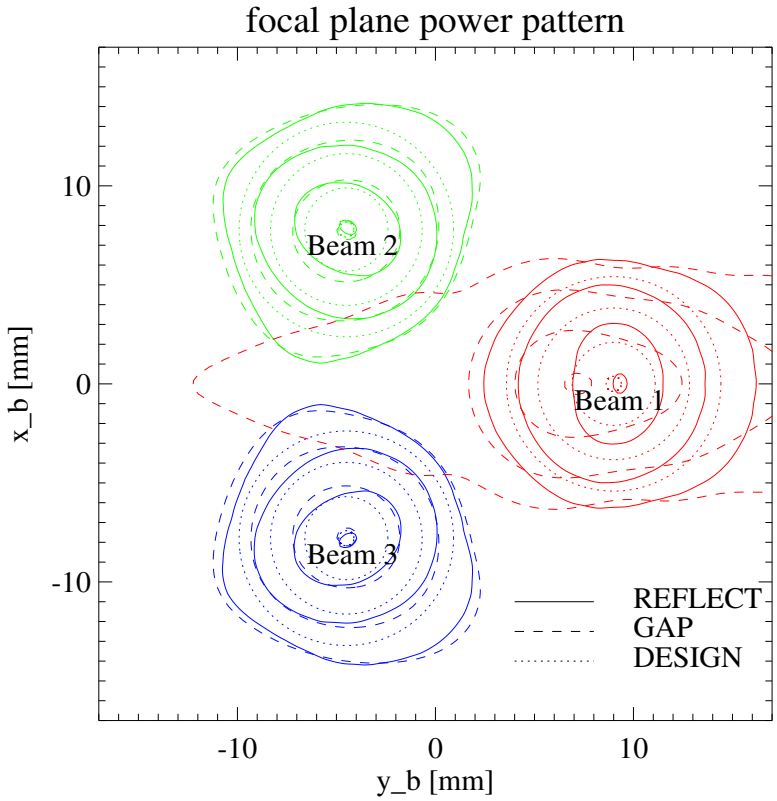

Figure 6: Expected power patterns in the focal plane of the telescope, the contours indicating the -0.1, -3, -10 and -20 dB levels. The solid and dashed lines show the results of simulations with REFLECT and GAP respectively. The dotted lines represent the beams following from the quasioptical design.

from the focal plane. This shift, however, should not have a significant influence on the result because a Gaussian beam with a waist radius $w_0 = 4.3$ mm would only expand by less than 7%.

There is a good agreement between our measurements and Pat Foster's simulations (Fig. 7). A similar agreement is found for the results of GAP if only beam 2 and 3 are considered. The relative positions of the beams correspond to the designed ones, there is just a slight displacement in the negative x-direction of $\sim$0.6 mm that might however well be due to alignment errors of the test setup. The beams also show a slight asymmetry which is different from the one seen in the simulations. On one hand this might be due to a polarisation effect, because for mechanical reasons the preliminary measurements had to be done in the po-

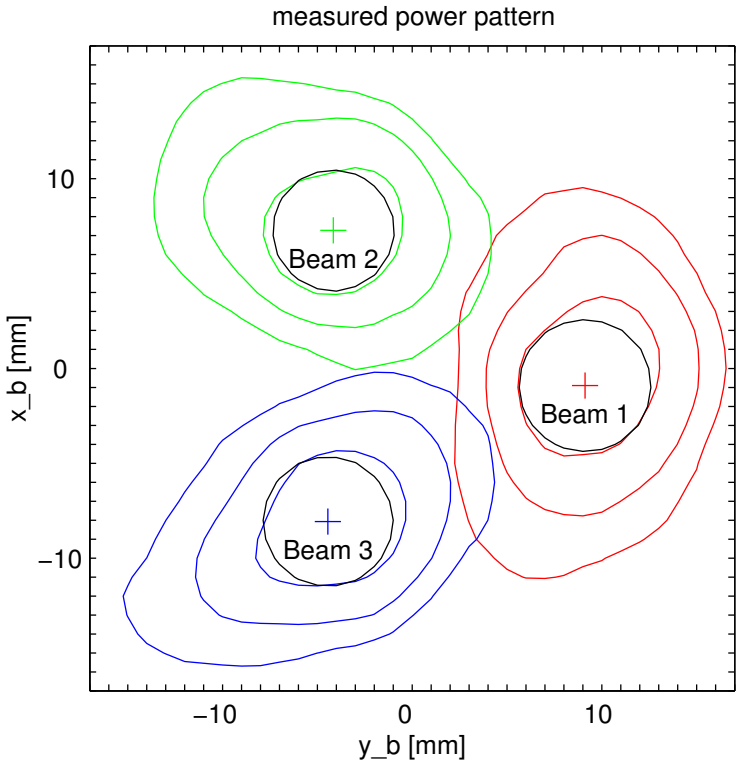

Figure 7: Measured (near field) focal plane power patterns. The contours indicate the -3, -10 and -20 dB levels, the crosses and black circles the centre and the -3 dB contours of Gaussian beams fitted into the measured data.

larisation orthogonal to the simulations with REFLECT. On the other hand the observed asymmetry might also be due to the damaged sample feedhorn. The strong asymmetry of beam 1 in the GAP-simulations is not observed at all. So far there is no explanation for GAP's poor performance concerning this special situation.

Into each measured power pattern a Gaussian beam was fitted, resulting in beam radii of $\sim$5.5 mm. Even taking into account beam broadening during propagation over 15 mm, this is considerably higher than the the designed value. This effect is probably due to the missing probe-correction: The waveguide-probe[3] leads to a broadening of the measured patterns. For the final measurements this must be taken into account in order to obtain correct results for the beam waist radii.

From the measured phase the direction of propagation can be determined, which is identical within 0.6 degrees for all three beams. The absolute difference from

[3]Waveguide dimensions: $\sim$ 0.5 by 1 mm

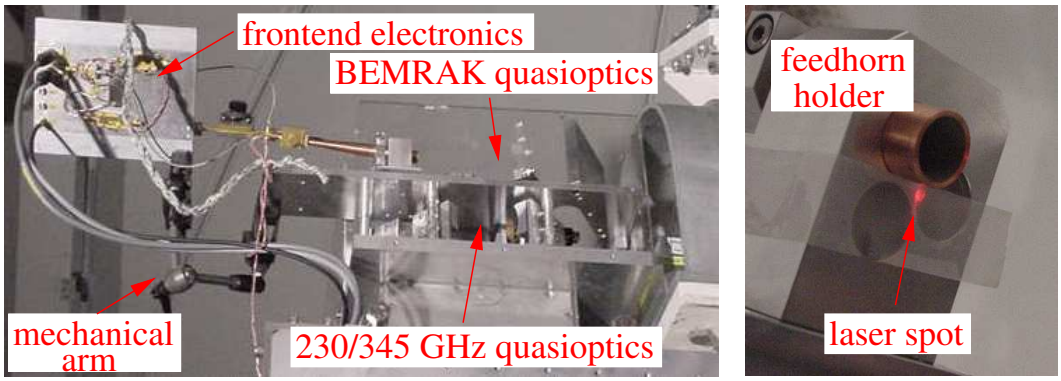

Figure 8: BEMRAK optics and front-end electronics integrated into the 230/345 GHz KOSMA-receiver. The laser beam that defines the telescope axis misses the centre of the feedhorn cluster (only one horn shown) by less than 2 mm, which is well within the tolerances of the quasioptical design.

the nominal telescope axis is less than 1.5 degrees and can probably be attributed to alignment errors in the test setup.
Final measurements will be made exactly in the focal plane for both polarisations (including the one used for simulations with REFLECT). In addition, the location of the beam-waists will be checked by measurements in parallel planes, looking for the one with minimum observed beam radii.

4.3 Integration into the KOSMA-telescope

BEMRAK is mounted onto the base plate of the 230/345 GHz KOSMA-receiver by several pillars (Fig. 3). As the CAD-drawings of KOSMA were available and our quasioptical design tolerates misalignments of up to $\sim$5 mm, no adjustment was planned. In fact, integration into the KOSMA-receiver went off without a hitch. The general adjustment was checked by using KOSMA's adjustment laser unit which sends a laser beam along the telescope axis. The wire grid was replaced by a dummy mirror so that the laser beam was reflected into BEMRAK. The laser spot appeared $\sim$1-2 mm from the centre of the dummy mirror and missed the centre of the feed horn cluster by the same distance (Fig. 8). The small misalignment was mainly in the plane parallel to the mounting plate, whereas the height was correct. If adjustment had to be done, it would be sufficient to allow only for lateral movements. But as will be seen later, this is not required.
The front-end electronics, consisting of the local-oscillator, the first intermediate frequency amplifiers and mixers, was mounted on the baseplate of BEMRAK by means of a mechanical arm (Fig. 8). This device could be twisted in all directions

and then be fixed by a single screw, thus providing the flexibility to test all three feedhorn positions with a single feedhorn/mixer chain.
The front- and backend electronics proved to be well adapted to the extreme climatic and electrostatic conditions at Gornergrat. They both worked flawlessly, and the temperature of the much-exposed front-end was stable, even when the telescope cupola was opened and the ambient temperature dropped rapidly to $\sim 0^{\circ}$C.
During installation an error was made regarding the orientation of the elliptical mirror. As it is almost symmetrical no side effects are expected. This was confirmed by near-field measurements and GAP-simulations of the telescope antenna pattern (far-field) above the -25 dB level. The measurements should therefore show the correct antenna beams.

4.4 Antenna beam patterns

The simulations with GAP resulted in antenna beams with a half power beam width (HPBW) of $\sim$1.6 arcmin that intersect each other at their -3.1 dB level (Fig. 9). The sidelobe level is below -17 dB. Despite the strong asymmetry in the field distribution of horn 1 in the focal plane of the telescope, no corresponding feature was seen in the far-field simulations.
For the antenna beam measurements a test-transmitter was tuned to the centre of the upper sideband of BEMRAK (212 GHz). It consists of a Gunn-oscillator followed by a tripler. The signal of the horn feed is focused by a 90 degree offset-parabolic mirror with a diameter of $\sim$120 mm which gives a HPBW of $\sim$1.2 degree [9]. It was installed on the top of 'Klein Matterhorn' which is the farthest point with any access in this high-mountain environment. Its distance from the telescope is approximately only half of the far-field distance so that far-field conditions are not fulfilled. Nevertheless, the difference to the "true" far field should be negligible [9].
Fortunately the lower-frequency (210-270 GHz) KOSMA-receiver could be tuned also to 212 GHz, so that it was possible to measure both beams simultaneously. At the beginning of the measurements the 330-365 GHz receiver also detected a signal at 354 GHz, which is the 5th harmonic of the Gunn frequency used in the test-transmitter. Later it vanished which is probably due to the increasing humidity of the atmosphere during this very warm and sunny day. Nevertheless, this opens the possibility of measuring all antenna beams simultaneously with a single test-transmitter. As the humidity during the summer months will be higher, it should however be tried to increase the 354 GHz signal by optimising the tripler for maximum power at the 5th harmonic[4]. During the preliminary antenna beam

[4]As the reconstruction of source position and size requires accurate knowledge of the antenna beam patterns, a decrease of the transmitted power at 212 GHz is not recommended. Retuning of

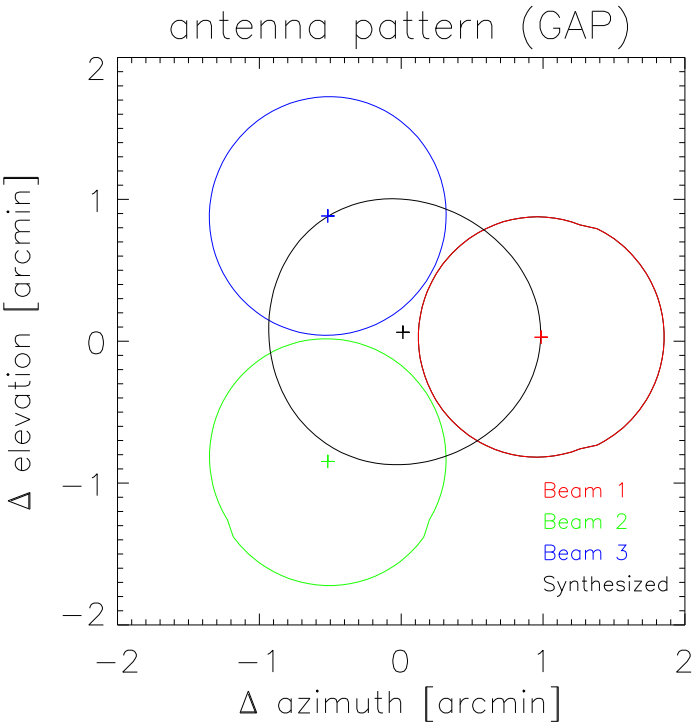

Figure 9: Contours at -3 dB from GAP-simulations. The black contour corresponds to the synthesised beam. The antenna patterns are shown in the azimuth/elevation coordinate system for the KOSMA-telescope pointing to an elevation of 0 degrees.

measurements under discussion no attempts were made to measure simultaneously at 354 GHz, as the mapping software for BEMRAK was not yet ready. Therefore the continuum backend (COBAC) of KOSMA had to be used which provides only two signal inputs: One for the 210-270 GHz KOSMA-receiver, the other for the single BEMRAK-channel.
For each of the three feedhorn positions two maps of 20 arcmin by 20 arcmin were obtained. The scan direction of the meander scans was in azimuth. Each map consists of 21 lines (each containing 200 sample points), which took the telescope $\sim$10 minutes to scan. For the final antenna beam measurements (when all beams can be measured simultaneously) this distance will be reduced to 10 arcsec, and in addition there will also be scans with the scan direction in elevation.

the transmitter in order to measure also the highest frequency beam pattern should be used only to check the alignment of all beams (which could also be accomplished by solar-scans).

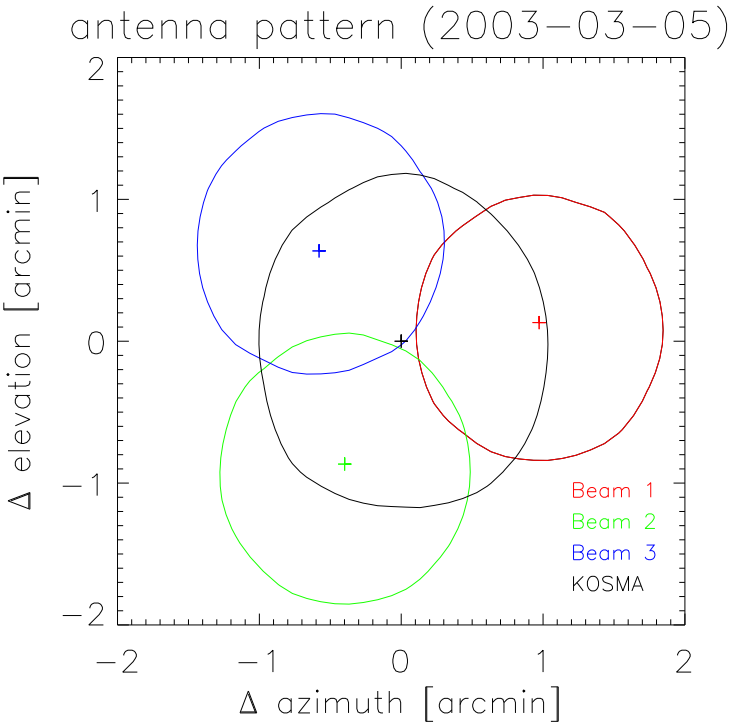

Figure 10: Measured -3db contours for the four BEMRAK- and KOSMA beams at 212 GHz. The crosses indicate the maxima of Gaussian fits to the measured power patterns. Note that the black contour does not represent the synthesised beam as in figure 9. The latter could not be measured with only one channel available.

The reproducibility of all beam-patterns is very good, down to below the -20 dB level. We therefore conclude that the influence of the atmosphere on these measurements can be neglected. This assumption is further supported by the fact that the weather was very sunny and constant with only a few cirrus clouds high above the test range. For the KOSMA-beam there is a total of six maps which are also almost identical and well aligned. Therefore the relative positions of the three BEMRAK-beams are believed to be correct.

The measured antenna patterns are shown in Figure 10. They have been rebinned to an array with 200 by 21 points by means of a cubic interpolation (IDL congrid-procedure) for display. Half-power beam-widths and beam positions were determined by fitting a Gaussian beam to the data (200 by 21 points). The HPBW are $\sim$1.6 arcmin in azimuth and $\sim$1.7 arcmin in elevation for BEMRAK and $\sim$2.0

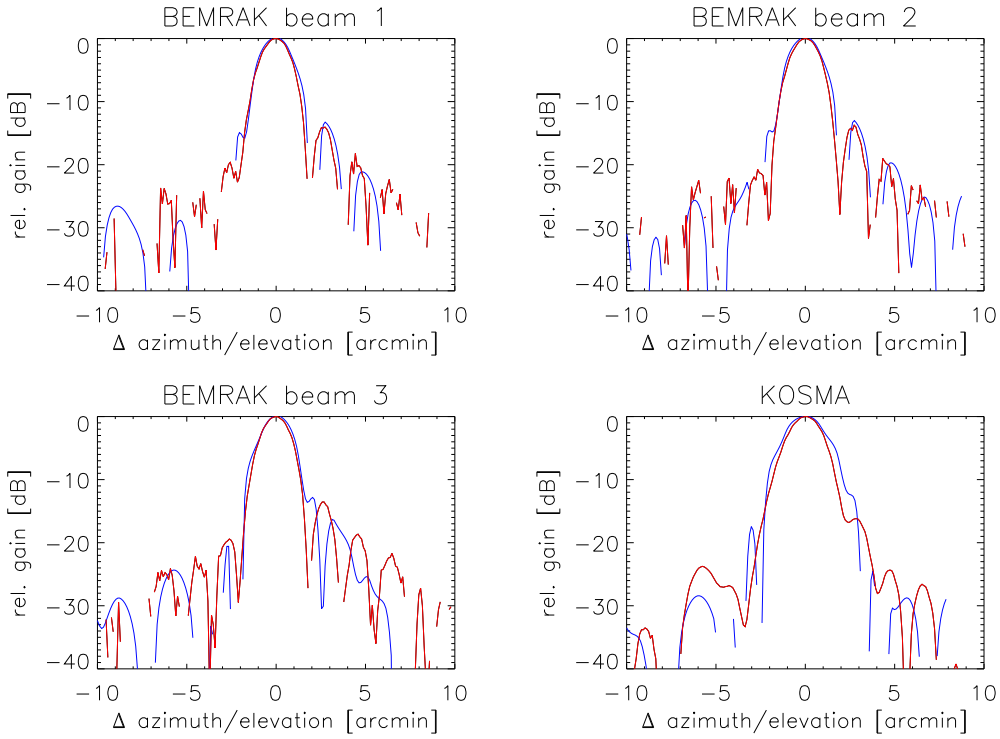

Figure 11: Measured far-field cuts for the three BEMRAK-beams and for the KOSMA-beam at 212 GHz after normalisation. The red patterns correspond to the azimuth direction, the blue ones to elevation.

and $\sim$ 2.3 arcmin for KOSMA respectively[5]. The values for BEMRAK are in good agreement with the GAP-simulations, whereas the HPBW of the KOSMA-beam agrees only in azimuth direction with the $\sim$2.0 arcmin measured earlier at 230 GHz [12]. The asymmetry in the KOSMA-beam occurs in the same direction as the slight one seen in the BEMRAK-beams, but is much stronger. The are two possible explanations for this: i) the wire grid introduces an asymmetry into all four beams, but affects the one from the KOSMA-receiver more strongly for unknown reasons, or ii) it is an effect of the 210-270 GHz KOSMA-receiver itself. An additional antenna scan without grid resulted in the KOSMA-receiver getting saturated, with no time left for a further scan. The effect of asymmetry will be investigated in detail during the final measurements.
The three BEMRAK-beams intersect at the -2.6 and -2.1 dB levels which is

[5]The difference between the HPBW of KOSMA and BEMRAK is explained by the different edge tapers of $\sim$14 and $\sim$2 dB. The latter value is too low for an efficient illumination of the telescope (leading to higher sidelobes), but is required for beams overlapping at -3 dB [9].

slightly higher than planned. As the HPBW corresponds to the designed one and the beams are almost symmetric, this effect is due to the relative beam positions. The latter form more or less an equilateral triangle (interior angles of 54, 61 and 65 degrees) as they do in the GAP-simulations (Fig. 9), but the angular distance between beam 2 and 3 is only $\sim$1.6 arcmin instead of the planned $\sim$1.75 arcmin. This triangle is rotated by $\sim$7 degrees anti-clockwise which corresponds to the Nasmyth-rotation (the elevation of the test-transmitter is $\sim$7 degrees). Alignment of the three BEMRAK-beams with the 212 GHz KOSMA-beam is very good, the difference of $\sim$0.1 arcmin between the centre of the BEMRAK-beams and the KOSMA-beam is well below the accuracy of the measurement.
The sidelobe level is higher than predicted by GAP-simulations: Figure 11 shows that the first sidelobes appear at -13 dB (instead of -17 dB). In addition there is an asymmetry in the sidelobe level which is not predicted by GAP, not even when the adjustment of BEMRAK was varied within the design tolerances, or when the elliptical mirror was mounted incorrectly (see section 4.3). The same asymmetry can also be found in the KOSMA-beam, with and without installed wire grid[6]. So far it is not clear whether this is an inherent effect of the telescope itself, a problem induced by BEMRAK even when the wire grid is not installed, or caused by reflections along the test range. As BEMRAK must not interfere with other astronomical observations, the original antenna patterns will be re-measured before final installation.
As expected, the measured KOSMA-beam corresponds more or less to the simulated synthesised beam, regarding the HPBW as well as its position. If synthesising of a fourth beam really became impossible, KOSMA's 230 GHz receiver could be tuned to 212 GHz and used as BEMRAK's fourth beam. One would then lose the 230 GHz spectral point, but the latter probably does not contain a lot of new information anyway when simultaneous observations at 212 GHz are available.

5 Conclusions

Calibration of solar flare observations from telescopes with narrow beams requires knowledge of source position and size. We have developed a new multibeam receiver at 210 GHz which will be integrated into the existing 230/345 GHz receiver of the KOSMA-telescope, allowing simultaneous observations at all three frequencies. BEMRAK consists of three radiometers, a fourth beam will be synthesised from the other three. The former is in the centre of the beam cluster, thus enlarging the field where unambiguous reconstruction of the source position and size is possible. In addition, this is a cost-effective way to realise a four-beam receiver.

[6] Although the KOSMA-receiver without the wire grid was temporarily in saturation, the sidelobes are well resolved.

Due to delivery problems and a pending repair of the 230/345 GHz KOSMA-receiver, final integration of BEMRAK will not be possible before mid-June. In order to test the receiver-design, when there was still time left for eventual modifications, the available single channel was used for near field measurements in the focal plane as well as for antenna beam measurements using a test transmitter. The preliminary measurements clearly show that

- the focal plane power patterns agree well with the design and the simulations with REFLECT. All three beams are at the intended positions, with nearly identical directions of propagation. The measured waist radii are $\sim$20% larger than the ones resulting from the simulation which is probably due to the (so far) missing probe-correction. The strong asymmetry seen in GAP-simulations for beam 1 is not present in the measured power pattern.
- integration into the KOSMA-telescope was without any complications. Although there is no means for adjustment, good alignment with the telescope was reached.
- the front- and backend electronics worked flawless under the extreme climatic and electrostatic conditions at this high-altitude environment.
- the test transmitter proved again to be easy to operate and very reliable with no need for adjustment. The emitted power was more than enough for the antenna beam measurements at the given distance between KOSMA and test transmitter (dynamic range of $\sim$30 dB even with the defective feedhorn).
- the 230 GHz KOSMA-receiver can be tuned to 212 GHz, thus allowing simultaneous measurement of all beams (except 345 GHz) with a single test-transmitter. If necessary this receiver could be used to produce the fourth beam for BEMRAK.
- the measured antenna patterns show the three BEMRAK-beams well aligned with the KOSMA-beam, thus both instruments can observe the same source.
- the BEMRAK-beams do not intersect exactly at the -3 dB-level, but this does not affect their usefulness for source location.
- the measured sidelobe level is slightly higher than in the simulations, but a similar effect is also seen in the KOSMA-beam. Therefore this might be an effect of the telescope itself.

We therefore conclude that BEMRAK works as specified. There is no need for modifications, neither concerning the quasioptics layout itself, nor any additional means for adjustment. However there are some points to be observed for the final measurements:

- The mapping software for our own measurement computer must be finished.

Only then it is possible to obtain all beam-patterns simultaneously. This is also an important precondition for solar observations.

- Before BEMRAK is installed again, the antenna patterns of the KOSMA-telescope alone should be measured. This allows to estimate if BEMRAK has a negative influence on the telescope performance. If so, it must be de-installed at the beginning of the winter observation-season.
- The scanning-scheme has to be altered: The distance between the scan lines will be reduced to 10 arcsec and there will be scans in azimuth as well as in elevation.
- In addition, the effect of subreflector scanning has to be investigated: In order to observe not only an activity region but also a quiet reference region on the solar disc, the beams are deflected by ± 3 degrees by means of a tiltable subreflector [12, 14]. The preliminary antenna pattern measurements were made with aligned subreflector.

A Solar Maps

Source positions can be obtained from solar maps, but as it takes the telescope $\sim$20 minutes to scan the full solar disc this offers no usable time resolution. Efforts to increase the "frame rate" were made in August 2002: The scan area was reduced to 10 arcmin by 10 arcmin, which would be enough for solar flare observations. But these small maps took $\sim$3 minutes. The only way to scan a comparable area of the solar disc at a higher cadence makes use of the subreflector wobble mechanism: The latter permits to move the antenna beam up to 6 arcmin in cross-elevation in only 70 ms. Combined with a periodic 6 arcmin up-and-down movement in elevation this would result in 6 arcmin by 6 arcmin maps. The achievable "frame rate" was estimated to 0.1 to 0.2/s. Two main problems were identified:

- There would be a substantial part (up to 50%!) of the time not usable for observations at all. This happens as it takes the telescope several seconds to reverse direction and reach the intended scan velocity. During this time there is no way of knowing the telescope position.
- The movement of the subreflector consists of three phases: Acceleration, linear movement and deceleration (Fig. 12). Most of the 6 arcmin scan is completed during the phase of linear movement. It lasts only $\sim$30 ms, i.e. about twelve times the integration constant τ_{RC}, which is determined by the KOSMA receivers and can not be shortened. To satisfy the Nyquist theorem, on a linear distance of 6 arcmin 7 and 9 independent samples should be taken at 230 and 345 GHz respectively. Due to the fast beam movement and the long integration time however, the samples would not be independent, leading to smoothed maps. The latter are difficult to analyse at best and completely worthless at worst. In any case, careful simulations of observations and the possible data analysis should be made before the effort of such observations is made.

B Specifications

- Telescope (Fig. 13)
  - General layout: Cassegrain system with two Nasmyth-ports
  - Main reflector diameter: 3000 mm
  - Main reflector focal length: 1300 mm
  - Subreflector diameter: 270 mm
  - Subreflector-hyperboloid: a_h = 1322.50 mm, b_h = 563.38 mm

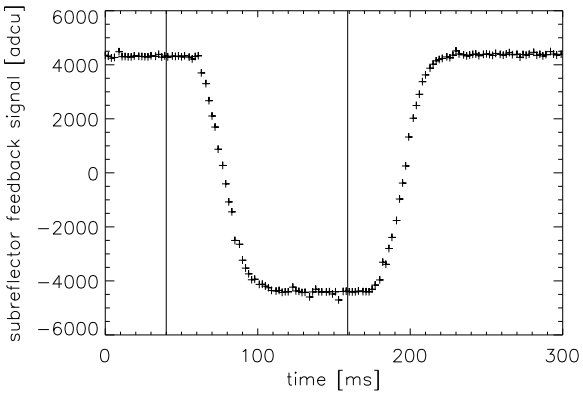

Figure 12: Feedback signal of the subreflector wobble-mechanism. The vertical lines indicate the times when the command to start movement was given.

  - Effective focal length: 31200 mm

- Elliptical mirror (Fig. 13)
  - Beam bending angle: 60 degrees
  - Projected mirror radius (r_{mirror}): 50 mm
  - Focal length: 106.25 mm
  - Focal distances: $R_{telescope}$ = 200.03 mm, R_{horn} = 226.64 mm
  - Input/output waist distances: $d_{telescope}$ =196.00 mm, d_{horn} = 220.81 mm
  - Input/output waist radii: $r_{telescope}$ = 3.57 mm, r_{horn} = 4.03 mm
  - Half axes of ellipsoid: a_e = 213.34 mm, b_e184.40 mm
- Feedhorns
  - General layout: Corrugated circular with sine-tapered walls
  - Aperture radius: 7.0 mm
  - Length: 140 mm
  - Beam waist radius: 4.03 mm (corresponding to a HPBW of 7.6 degrees)
  - Feedhorn positions and separation determined by geometrical ray-tracing
  - Feedhorn tilts relative to central ray of cluster:

Feedhorn	α (horizontal) [deg]	β (vertical) [deg]
1	4.8	0.0
2	-2.6	4.2
3	-2.6	-4.2

Table 1: Feedhorn tilts relative to central ray of cluster.

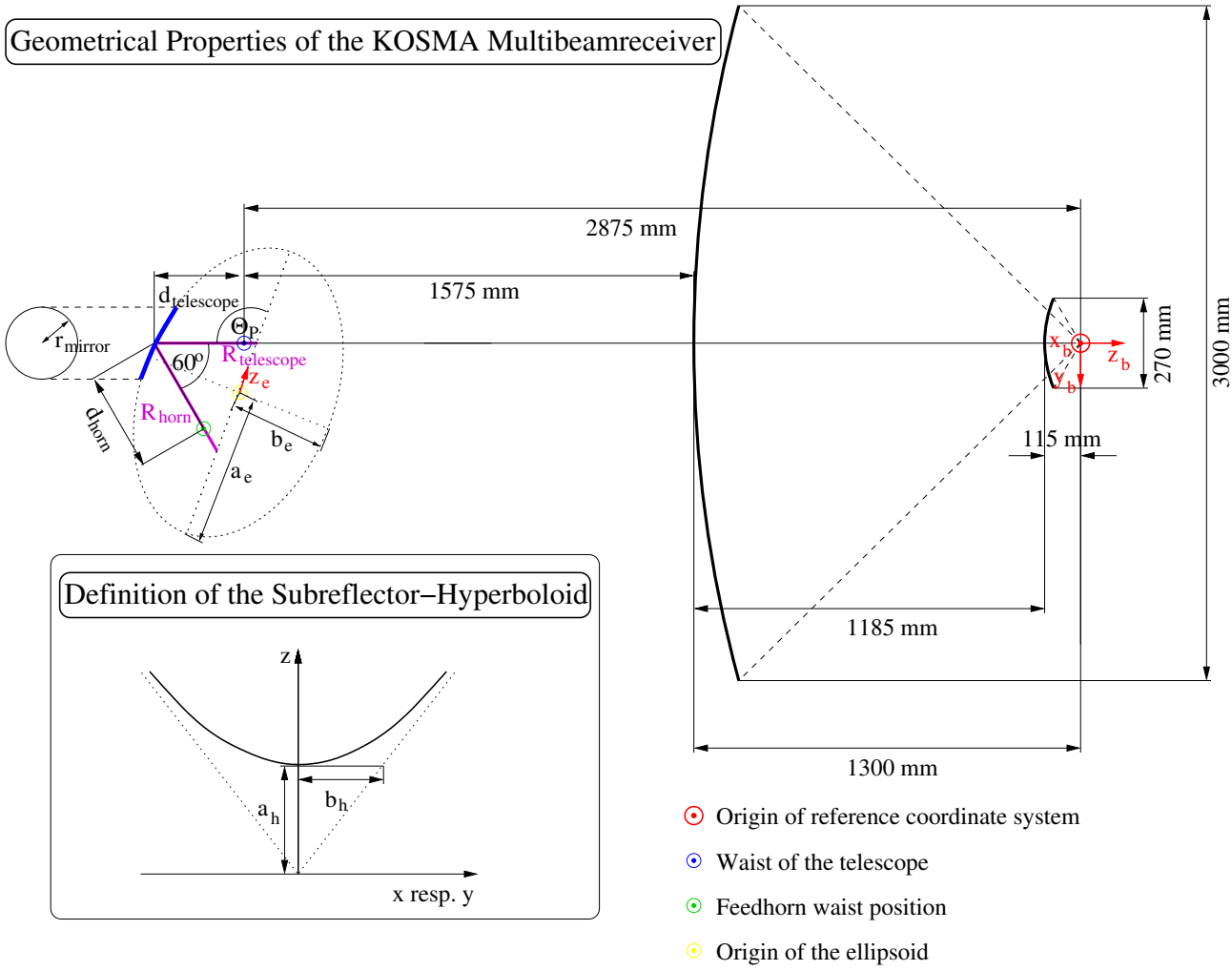

Figure 13: Geometrical properties of the KOSMA-telescope and BEMRAK's elliptical mirror. For simplicity the telescope's (flat) tertiary mirror is omitted. Missing properties are given in the text.

- Simulated antenna patterns (GAP)
  - HPBW (beam 1 to 3): 1.6 arcmin
  - HPBW (synthesised beam): 1.9 arcmin
  - Beam 1 to 3 overlapping at: -3.1 dB
  - Sidelobe level: $\lesssim$-17 dB
- Radiometric properties of the multibeam receivers
  - Centre frequency: 210.6 GHz
  - Intermediate frequency range: (1.4$\pm$0.25) GHz, DSB
  - Receiver noise Temperature: $\sim$3000 K
  - Integration constant: 2.3 ms (as KOSMA's 230/345 GHz receiver)
  - Radiometric sensitivity: $\sim$3.7 K ($\hat{\approx}$0.17 sfu)

Acknowledgements

This work is funded by the Swiss National Science Foundation.

References

[1] C. G. Gimenez de Castro, J.-P. Raulin, V. S. Makhmutov, P. Kaufmann, and J. E. R. Costa, "Instantaneous positions of microwave solar bursts: Properties and validity of the multiple beam observations", Astron. Astrophys. Suppl. Ser. **140**, 373-382, 1999.

[2] V. A. Efanov, and I. G. Moiseev, "The Observational Method of Solar Radio Emission Bursts by Sharp-Directional Aerials", Russian Academy of Science, Moscow 1967

[3] J. E. R. Costa et al., "A Method for Arc-Second Determination of Solar Burst Emission Centers with High Time Resolution and Sensitivity at 48 GHz", Solar Physics, **159**, 157-171,1995.

[4] L. L. Croom, "Solar Flux Levels at Frequencies Above 10 GHz and Slough Millimetre Solar Observatory Burst Intensities", Science Research Council, Appleton Laboratory, Ditton Park, Slough SL3 9JX, England, 1979

[5] P. Foster, "Nearfield for KOSMA Feeds", MAAS Report 492 Issue No 1, 2002

[6] P. F. Goldsmith, "Quasioptical Systems", Institute of Electrical and Electronical Engineers, Inc., New York, 1998

[7] R. Herrmann, A. Magun, J. E. R. Costa, E. Correia and P. Kaufmann, "A multibeam antenna for solar mw-wave burst observations with high spatial and temporal resolution", Solar Physics, **142**,157-170, 1992.

[8] C. Kramer, J. Stutzki, "Atmospheric Transparency at Gornergrat", Technical Memorandum No. 5, 1990
http://www.ph1.uni-koeln.de/gg/tech_rep/05_wetter/tb5tb5.html

[9] A. Lüdi, "Solares Submillimeterteleskop: Berechnungen und theoretische Betrachtungen zur Antenne", Diplomarbeit an der Universität Bern, 1998

[10] A. Lüdi, and A. Magun, "Antenna-pattern-measurements of the solar submm telescope at 212 and 405 GHz, Tech. rep. IAP 99-3, Inst. of Appl. Phys., Bern, 1999

[11] A. Lüdi and A. Magun, "Near-horizontal line-of-sight millimeter-wave propagation measurements for the determination of outer length scales and

anisotropy of turbulent refractive index fluctuations in the lower troposphere“, Radio Science, **37(2)**,12-1 - 12-19, doi:10.1029/2001RS002493, 2002.

[12] T. Lüthi, ”Rekonstruktion der Flussdichte des Flares vom 12. April 2001 bei 230 und 345 GHz“, IAP-Forschungsbericht Nr. 2002-6, Bern, 2002

[13] T. Lüthi and Axel Murk, ”Doppelseitenbandbetrieb eines Nulling-Interferometers zur Beobachtung von solaren Flares“, IAP-Forschungsbericht Nr. 2002-17, Bern, 2002

[14] T. Lüthi and A. Magun, ”First observation of a solar X-class flare in the submillimeter range with KOSMA“, submitted to Astron. Astrophys., 2003